Eurographics Conference on Visualization (EuroVis) (2012)
M. Meyer and T. Weinkauf (Editors)

Calibration of the Marschner-Lobb Signal on CC, BCC, and FCC Lattices

Viktor Vad[1], Balázs Csébfalvi[2], Moncef Gabbouj[1]

[1]Tampere University of Technology, Finland
[2]Budapest University of Technology and Economics, Hungary

Abstract

The well-known Marschner-Lobb (ML) signal has been originally proposed for visually comparing 3D resampling filters applied on the traditional Cartesian Cubic (CC) lattice. Recently, this popular benchmark is also used for evaluating reconstruction schemes designed for the optimal Body-Centered Cubic (BCC) lattice and the suboptimal Face-Centered Cubic (FCC) lattice. Nevertheless, to the best of our knowledge, it has not been thoroughly studied whether the ML signal meets the assumptions that the theory of optimal regular volume sampling is based on. In this paper, we try to find equivalent CC, BCC, and FCC representations for unbiased comparisons. For the continuous reconstruction, we use comparable approximations of the ideal low-pass filter, and increase the sampling frequency until the aliasing effects completely vanish. Based on these experiments, we show that the ML signal is appropriate for comparing the CC and BCC lattices, but it is inappropriate for fairly comparing the FCC lattice to the CC and BCC lattices regarding the visual quality of the corresponding reconstructions. In fact, the ML signal very strongly prefers the FCC sampling due to the special shape of its spectrum. However, this property can hardly be expected from a practical signal.

Categories and Subject Descriptors (according to ACM CCS): I.3.3 [Computer Graphics]: Picture/Image Generation—Display algorithms I.4.10 [Image Processing and Computer Vision]: Image representation—Volumetric

1. Introduction

From a signal-processing point of view, direct volume rendering can be interpreted as a 3D resampling task, where the initial discrete volume representation has to be resampled at evenly spaced sample positions along the viewing rays. If the voxels represent samples of the underlying signal on a specific lattice, the resampling is performed as a convolution of the discrete samples with a continuous filter kernel. The applied reconstruction filter strongly influences the quality of the rendered images. On one hand, filters of high approximation order are required to achieve high numerical accuracy [MMMY96, MMMY97b]. On the other hand, in volume visualization applications, the reduction of visual artifacts also plays a crucial role. Therefore, different reconstruction schemes are usually compared empirically on synthetic or measured data sets. A comparison on practical data is somewhat problematic, as it is not known exactly how well the acquired data represents the underlying signal. Consequently, it is difficult to determine how much the artifacts are due to the imperfect reconstruction filter or the imperfect data acquisition. To analyze reconstruction filters in terms of visual quality independently from the data acquisition, Marschner and Lobb analytically defined a 3D test signal [ML94]. Although this signal is not band-limited, above a practical Nyquist limit, it contains frequency components of minimal amplitude. However, right below this practical Nyquist limit, relatively high energy is concentrated. Therefore, the reconstruction of the Marschner-Lobb (ML) signal from its discrete samples is a challenging task. The ML signal is a widely accepted benchmark (cited more than 250 times), since it is appropriate for testing the visual quality of different reconstruction schemes in terms of oversmoothing (or detail preservation as opposed to oversmoothing), postaliasing, and isotropy at the same time.

The ML signal was originally recommended for comparing reconstruction filters applied on the traditional CC lattice. Recently, reconstruction schemes proposed for the optimal BCC lattice and the suboptimal FCC lattice were

DOI: 10.2312/PE/EuroVisShort/EuroVisShort2012/019-023

also analyzed by ML experiments [EDM04, CH06, Csé10, EVDVM08, MES*11, ME10, ME11]. However, we think that these experiments need to be substantiated by a precise validation of the ML signal for the BCC and FCC lattices. To the best of our knowledge, such a validation has not been published yet. Furthermore, it has not been thoroughly investigated how the sampling frequency has to be set to obtain equivalent CC, BCC, and FCC representations of the ML signal. If the sampling frequency is not sufficient, it leads to prealiasing effects that could hardly be distinguished from the postaliasing effect of a practical reconstruction filter. Therefore, the visual comparison of Cartesian and non-Cartesian reconstruction schemes might potentially be misleading.

2. Related Work

Since 1994 [ML94], in the literature on volume reconstruction, one could hardly find a paper that does not contain an evaluation on the ML signal. Especially interpolation and derivative filters [MMMY96, MMK*98, MMMY97a, THG00, Csé08, CD09b] can be compared depending on how accurately they can reproduce the isosurfaces and the gradients of the ML signal, respectively. Visual comparisons were similarly made between spatial-domain and frequency-domain resampling methods [AMVG05, LME04, CD09a]. The ML signal was used also for analyzing the visual quality of irregular volume rendering [LGM*08] as well as isosurface extraction [CMS01, CTM03, ABJ05, MKRG11] and refinement [Ber04] techniques.

2.1. Volume Sampling on Non-Cartesian Lattices

In the last decade, reconstruction filtering on the optimal BCC lattice and on the suboptimal FCC lattice received increased attention. Besides the theoretical substantiation, the superiority of the BCC and FCC lattices over the traditional CC lattice has been also confirmed by sampling the ML signal on these lattices and making visual comparisons of theoretically equivalent reconstructions [EDM04, CH06, EVDVM08, MES*11, ME10, ME11]. On the CC lattice, Marschner and Lobb suggested to take 40^3 samples from the interval $[-1,1]^3$ [ML94], since this sampling frequency guarantees that the passband contains 99.8% of the energy of the ML signal. Considering the ML spectrum to be spherically band-limited in a practical sense, equivalent BCC and FCC representations are supposed to consist of 29.3% and 23% fewer samples [PM62, TMG01], respectively. Nevertheless, in this paper, we demonstrate that the ML signal gives an unfair advantage to the FCC lattice when it is compared to the CC and BCC lattices (see Figure 1). Thus, the ML experiments do not justify that the FCC sampling ensures the lowest aliasing in general as suggested in recent comparative studies [ME10, ME11, YE11].

3. Calibration of the ML Signal on the CC Lattice

In the spatial domain, the ideal low-pass filtering can hardly be performed because of the infinite extent of the sinc kernel. Alternatively, the sinc interpolation can be implemented in the frequency domain [LME04, AMVG05], but it assumes a non-band-limited periodic extension. Therefore, assuming a real extension (i.e., taking the real discrete samples of the test signal outside the interval $[-1,1]^3$), we implemented highly accurate approximations of the sinc interpolation, by using very large Lanczos filters.

The Lanczos filter [TG90] is defined as follows:

$$L(t) = \begin{cases} sinc(t)sinc(t/a) \text{ if } |x| < a \\ 0 \text{ otherwise,} \end{cases} \quad (1)$$

where parameter a is an integer controlling the size of the filter kernel. The larger the value of a, the better the ideal sinc kernel is approximated.

For the isosurface rendering, we implemented a high-quality first-hit ray caster on the GPU using CUDA. This implementation provided reasonable rendering times for our experiments even though we used computationally expensive reconstruction filters for resampling along the viewing rays. Figure 1 shows the reconstruction of the ML signal from 40^3 CC samples applying a Lanczos filter with $a = 12$. Although such a large Lanczos kernel very well approximates the ideal low-pass filter, aliasing artifacts are still introduced. These artifacts can be caused by either prealiasing or postaliasing [ML94]. The prealiasing effect is due to the insufficient sampling frequency, while the postaliasing effect is due to the imperfect approximation of the ideal low-pass filter. In order to ensure that the discrete representation itself does not introduce a prealiasing effect, we increased the sampling frequency until the aliasing artifacts completely disappeared. Similarly to the previous papers, the sampling frequency is characterized by the number of voxels taken from the interval $[-1,1]^3$. Figure 2 shows that the resolution 45^3 still leads to a very slight oscillation of the outer rings. This oscillation vanishes at resolution 46^3. Increasing the number of CC samples from 46^3 to 47^3 does not make a visible difference. Thus, to eliminate the prealiasing effect, a resolution of 46^3 is already sufficient.

4. Calibration of the ML Signal on the BCC and FCC Lattices

For proper sampling on the BCC and FCC lattices, we applied a similar calibration as for the CC lattice. The Lanczos filter has been recently adapted to non-Cartesian lattices [YE11]. To obtain prealiasing-free BCC and FCC representations of the ML signal, we used the corresponding Lanczos filter adaptations. Just as for the CC calibration, we applied sufficiently large filters for the continuous reconstruction, and increased the sampling frequency until the prealiasing effect completely disappeared. Alternatively,

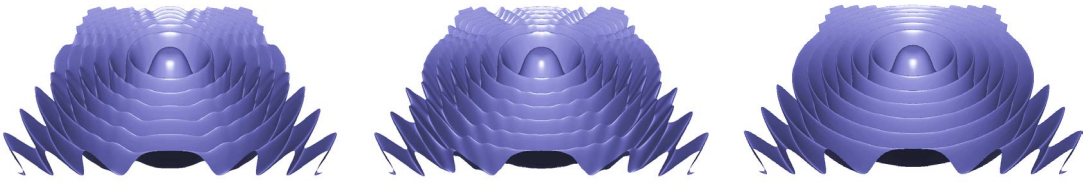

40^3 CC samples. $28^3 \times 2$ BCC samples. $23^3 \times 4$ FCC samples.

Figure 1: *Reconstruction of the ML signal using large Lanczos filters. The ratios between the number of samples are set such that the obtained CC, BCC, and FCC representations are equivalent according to the theory of optimal regular volume sampling [PM62,TMG01], which assumes that the original signal is spherically band-limited. However, the FCC representation still seems to be superior over the CC and BCC representations.*

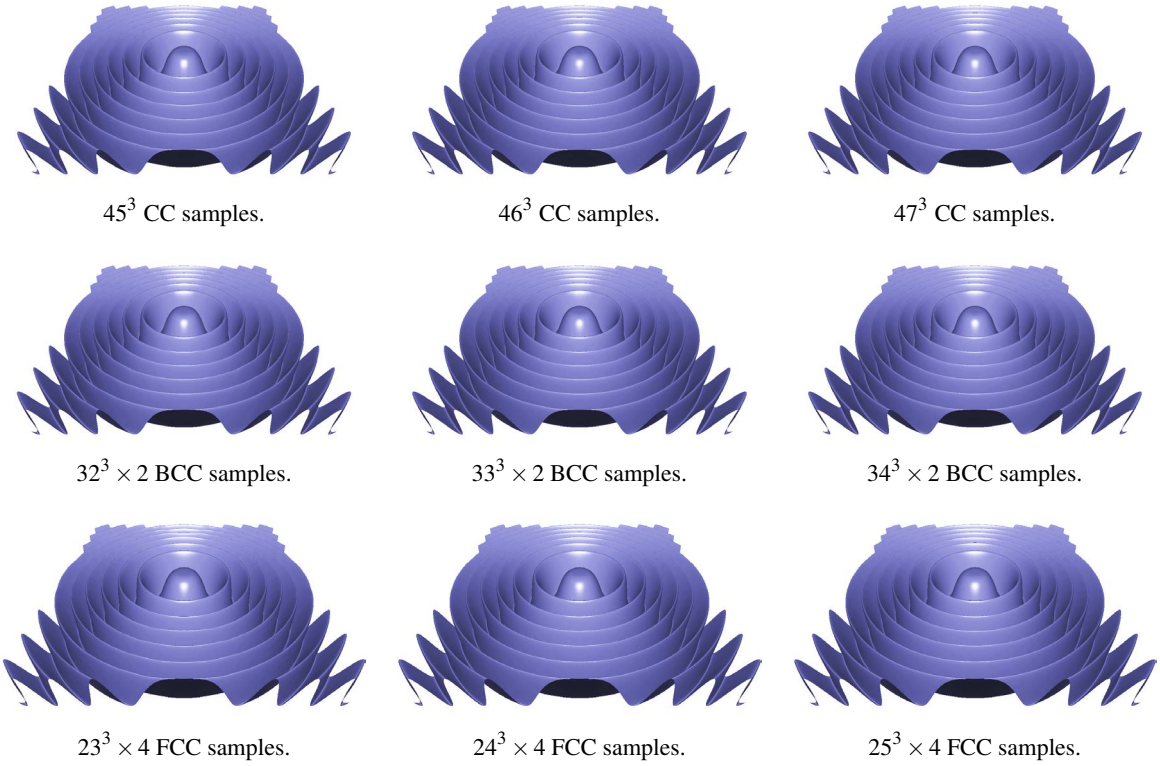

45^3 CC samples. 46^3 CC samples. 47^3 CC samples.

$32^3 \times 2$ BCC samples. $33^3 \times 2$ BCC samples. $34^3 \times 2$ BCC samples.

$23^3 \times 4$ FCC samples. $24^3 \times 4$ FCC samples. $25^3 \times 4$ FCC samples.

Figure 2: *Calibration of the ML signal on the CC, BCC, and FCC lattices. The middle column shows equivalent prealiasing-free representations.*

equivalent ML representations could be obtained by searching for resolutions that guarantee approximately the same reconstruction error. However, this strategy does not ensure that all representations are free from prealiasing, since the smoothing effect of the applied reconstruction filters contributes differently to the approximation error on the different lattices. The results of our calibration are shown in Figure 2. On the BCC and FCC lattices, resolutions of $33^3 \times 2$ and $24^3 \times 4$ already guarantee prealiasing-free reconstructions, respectively. Note that, compared to the CC sampling, the BCC sampling of the ML signal provides approximately the same reduction of samples that one can expect from the theory of optimal regular volume sampling ($33^3 \times 2/46^3 = 0.738 \approx 0.707$). On the other hand, the FCC lattice provides a significantly higher sampling efficiency than it is expected ($24^3 \times 4/46^3 = 0.5681 \ll 0.77$). This means that the ML signal prefers the suboptimal FCC sampling rather than the optimal BCC sampling. However, in the following section,

we theoretically justify that the preference of the FCC lattice has nothing to do with the assumptions of optimal regular volume sampling, but it is more related to the special shape of the ML spectrum.

5. Optimal Sampling of the ML Signal on the BCC and FCC Lattices

The ML signal [ML94] is defined as

$$\rho(x,y,z) = \rho_1(x,y,z) + \rho_2(x,y,z), \tag{2}$$

where

$$\rho_1(x,y,z) = \frac{1-\sin(\pi z/2)}{2(1+\alpha)},$$

$$\rho_2(x,y,z) = \frac{\alpha(1+\rho_r(\sqrt{x^2+y^2}))}{2(1+\alpha)},$$

and $\rho_r(r) = \cos(2\pi f_M \cos(\pi r/2))$. The parameters are set as $f_M = 6$ and $\alpha = 0.25$. The Fourier transform of $\rho_1(x,y,z)$ is $\hat{\rho}_1(\nu_x,\nu_y,\nu_z) = \frac{2}{5}\delta(\nu_x)\delta(\nu_y)(\frac{i}{2}\delta(\nu_z-\frac{1}{4})+\delta(\nu_z)-\frac{i}{2}\delta(\nu_z+\frac{1}{4}))$. Thus, this component of the spectrum consits of three Dirac impulses located along the z-axis. Since $\rho_2(x,y,z)$ does not depend on the value of z, its Fourier transform $\hat{\rho}_2(\nu_x,\nu_y,\nu_z)$ is non-zero only in the $\nu_x\nu_y$ plane ($\hat{\rho}_2$ is modulated by $\delta(\nu_z)$). Additionally, $\hat{\rho}_2$ is circularly symmetric and practically band-limited [ML94]. Therefore, the spectrum of the ML signal, which is dominated by $\hat{\rho}_2$, is disc-shaped.

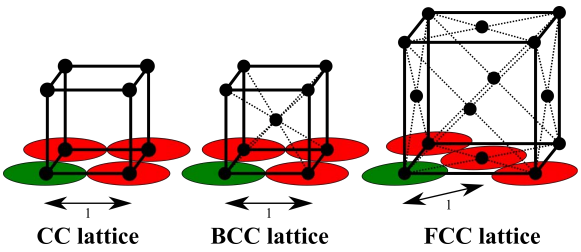

Figure 3: *Optimal arrangement of a disc-shaped spectrum on different lattices. The green disc depicts the primary spectrum, whereas the red discs depict the aliasing spectra. As the BCC lattice is the dual of the FCC lattice, in case of FCC sampling, the primary spectrum is replicated around the points of the dual BCC lattice. Vice versa, in case of BCC sampling, the primary spectrum is replicated around the points of the dual FCC lattice.*

If the ML signal is sampled on a certain lattice in the spatial domain, its disc-shaped spectrum is replicated around the points of the dual lattice (see Figure 3) in the frequency domain. However, to avoid prealiasing, the discs should not overlap. Furthermore, the tightest arrangement of the discs ensures the sparsest sampling in the spatial domain. Based on Figure 3, it is easy to see that the BCC lattice guarantees the densest disc packing, since it contains twice as many lattice points per unit volume as the CC lattice. In contrast, the FCC lattice contains just around 1.4142 times more lattice points per unit volume than the CC lattice (the FCC lattice consists of four interleaved CC lattices of edge length $\sqrt{2}$, thus its density is $4/\sqrt{2}^3 \approx 1.4142$). As the FCC lattice is the dual of the BCC lattice, it is more efficient for sampling the ML signal than the BCC lattice, which is proven to be optimal for the spherically band-limited scenario [PM62, TMG01].

Note that the sampling efficiency of the BCC lattice is exactly the same for a spherically band-limited signal as for a signal of a disc-shaped spectrum (the scaling of the dual FCC lattices for these two cases is the same). Therefore, the ML signal is a valid benchmark for testing BCC-based reconstruction schemes. However, on the FCC lattice, 50% fewer samples have to be taken from the ML signal than on a CC lattice to guarantee a prealiasing-free volume representation. This ratio is significantly better than the gain of 23% derived for spherically band-limited signals. As a consequence, the ML signal is not appropriate for comparing the FCC lattice to the CC or BCC lattices regarding the visual quality of the corresponding reconstructions, since due to its disc-shaped spectrum, it gives an unfair advantage to the FCC lattice.

6. Conclusion

The ML signal has been used for evaluating a variety of volume reconstruction techniques. Nevertheless, in this paper, we emphasized the importance of its validation for non-Cartesian reconstruction schemes. For the CC, BCC, and FCC lattices, we proposed a calibration method that can be used to obtain prealiasing-free volume representations. Interestingly, the suboptimal FCC representation provided the best sampling efficiency. However, we have theoretically justified that the ML signal strongly prefers the FCC sampling, but mainly due to the special shape of its spectrum. Therefore, we think that the previously published experiments on FCC-sampled ML representations are rather biased, and do not confirm that the FCC sampling ensures the lowest aliasing in general. Since, compared to the CC lattice, the higher sampling efficiency of the BCC and FCC lattices is derived from the reasonable assumption that the underlying signal is spherically band-limited (i.e., the spectrum does not contain preferred directions), a rigorous comparison of FCC and BCC volume representations requires a test signal that better meets this assumption, and does not give an advantage to either lattice. In our future work, we plan to find such a test signal.

Acknowledgements

This work was supported by the project TÁMOP-4.2.2.B-10/1–2010-0009 and OTKA 101527.

References

[ABJ05] ANDERSON J. C., BENNETT J., JOY K.: Marching diamonds for unstructured meshes. In *Proceedings of IEEE Visualization* (2005), pp. 423–429. 2

[AMVG05] ARTNER M., MÖLLER T., VIOLA I., GRÖLLER M. E.: High-quality volume rendering with resampling in the frequency domain. In *Proceedings of Joint EUROGRAPHICS-IEEE VGTC Symposium on Visualization (EuroVis)* (2005), pp. 85–92. 2

[Ber04] BERTRAM M.: Volume refinement fairing isosurfaces. In *Proceedings of IEEE Visualization* (2004), pp. 449–505. 2

[CD09a] CSÉBFALVI B., DOMONKOS B.: Frequency-domain upsampling on a body-centered cubic lattice for efficient and high-quality volume rendering. In *Proceedings of Vision, Modeling, and Visualization* (2009), pp. 225–232. 2

[CD09b] CSÉBFALVI B., DOMONKOS B.: Prefiltered gradient reconstruction for volume rendering. *Journal of WSCG 17*, 1-3 (2009), 49–56. 2

[CH06] CSÉBFALVI B., HADWIGER M.: Prefiltered B-spline reconstruction for hardware-accelerated rendering of optimally sampled volumetric data. In *Proceedings of Vision, Modeling, and Visualization* (2006), pp. 325–332. 2

[CMS01] CARR H., MÖLLER T., SNOEYINK J.: Simplicial subdivisions and sampling artifacts. In *Proceedings of IEEE Visualization* (2001), pp. 99–106. 2

[Csé08] CSÉBFALVI B.: An evaluation of prefiltered reconstruction schemes for volume rendering. *IEEE Transactions on Visualization and Computer Graphics 14*, 2 (2008), 289–301. 2

[Csé10] CSÉBFALVI B.: An evaluation of prefiltered B-spline reconstruction for quasi-interpolation on the body-centered cubic lattice. *IEEE Transactions on Visualization and Computer Graphics 16*, 3 (2010), 499–512. 2

[CTM03] CARR H., THEUSSL T., MÖLLER T.: Isosurfaces on optimal regular samples. In *Proceedings of Joint EUROGRAPHICS-IEEE TCVG Symposium on Visualization* (2003), pp. 39–48. 2

[EDM04] ENTEZARI A., DYER R., MÖLLER T.: Linear and cubic box splines for the body centered cubic lattice. In *Proceedings of IEEE Visualization* (2004), pp. 11–18. 2

[EVDVM08] ENTEZARI A., VAN DE VILLE D., MÖLLER T.: Practical box splines for reconstruction on the body centered cubic lattice. *IEEE Transactions on Visualization and Computer Graphics 14*, 2 (2008), 313–328. 2

[LGM*08] LEDERGERBER C., GUENNEBAUD G., MEYER M., BACHER M., PFISTER H.: Volume MLS ray casting. *IEEE Transactions on Visualization and Computer Graphics 14*, 6 (2008), 1539–1546. 2

[LME04] LI A., MUELLER K., ERNST T.: Methods for efficient, high quality volume resampling in the frequency domain. In *Proceedings of IEEE Visualization* (2004), pp. 3–10. 2

[ME10] MIRZARGAR M., ENTEZARI A.: Voronoi splines. *IEEE Transactions on Signal Processing 58*, 9 (2010), 4572–4582. 2

[ME11] MIRZARGAR M., ENTEZARI A.: Quasi interpolation with voronoi splines. *IEEE Transactions on Visualization and Computer Graphics 17*, 12 (2011), 1832–1841. 2

[MES*11] MENG T., ENTEZARI A., SMITH B., MÖLLER T., WEISKOPF D., KIRKPATRICK A. E.: Visual comparability of 3D regular sampling and reconstruction. *IEEE Transactions on Visualization and Computer Graphics 17*, 10 (2011), 1420–1432. 2

[MKRG11] MARINC A., KALBE T., RHEIN M., GOESELE M.: Interactive isosurfaces with quadratic C1 splines on truncated octahedral partitions. In *Proceedings of Conference on Visualization and Data Analysis* (2011). 2

[ML94] MARSCHNER S., LOBB R.: An evaluation of reconstruction filters for volume rendering. In *Proceedings of IEEE Visualization* (1994), pp. 100–107. 1, 2, 4

[MMK*98] MÖLLER T., MUELLER K., KURZION Y., MACHIRAJU R., YAGEL R.: Design of accurate and smooth filters for function and derivative reconstruction. In *Proceedings of IEEE Symposium on Volume Visualization* (1998), pp. 143–151. 2

[MMMY96] MÖLLER T., MACHIRAJU R., MUELLER K., YAGEL R.: Classification and local error estimation of interpolation and derivative filters for volume rendering. In *Proceedings of IEEE Symposium on Volume Visualization* (1996), pp. 71–78. 1, 2

[MMMY97a] MÖLLER T., MACHIRAJU R., MUELLER K., YAGEL R.: A comparison of normal estimation schemes. In *Proceedings of IEEE Visualization* (1997), pp. 19–26. 2

[MMMY97b] MÖLLER T., MACHIRAJU R., MUELLER K., YAGEL R.: Evaluation and design of filters using a Taylor series expansion. *IEEE Transactions on Visualization and Computer Graphics 3*, 2 (1997), 184–199. 1

[PM62] PETERSEN D. P., MIDDLETON D.: Sampling and reconstruction of wave-number-limited functions in n-dimensional Euclidean spaces. *Information and Control 5*, 4 (1962), 279–323. 2, 3, 4

[TG90] TURKOWSKI K., GABRIEL S.: Filters for common resampling tasks. In *Graphics Gems I* (1990), Glassner A. S., (Ed.), Academic Press, pp. 147–165. 2

[THG00] THEUSSL T., HAUSER H., GRÖLLER M. E.: Mastering windows: Improving reconstruction. In *Proceedings of IEEE Symposium on Volume Visualization* (2000), pp. 101–108. 2

[TMG01] THEUSSL T., MÖLLER T., GRÖLLER M. E.: Optimal regular volume sampling. In *Proceedings of IEEE Visualization* (2001), pp. 91–98. 2, 3, 4

[YE11] YE W., ENTEZARI A.: A geometric construction of multivariate sinc functions. *to appear in IEEE Transactions on Image Processing* (2011). 2